HEFAT2012
9th International Conference on Heat Transfer, Fluid Mechanics and Thermodynamics
16 – 18 July 2012
Malta

EXPERIMENTAL INVESTIGATION OF AL_2O_3-EG NANOFLUID THERMAL PROPERTIES AND HEAT EXPOSURE STABILITY IN CLOSED CIRCUIT

[1]*Hachey, M.- A., [1]Nguyen, C. T., [2]Galanis, N., [3]Popa, Catalin V.
*Author for correspondence

[1]Dept Mechanical Engineering, Faculty of Engineering, Université de Moncton, NB, Canada E1A 3E9
[2]Dept Mechanical Engineering, Faculty of Engineering, Université de Sherbrooke, Québec, Canada J1K 2R1
[3]GRESPI/Thermomécanique, Université de Reims Champagne–Ardenne, PO Box 1039, 51687 Reims, France
E-mail: marc.a.hachey@gmail.com

ABSTRACT

In the present study, we seek to further advance nanofluid research by simultaneously acquiring the thermal (thermal conductivity) and rheological (dynamic viscosity) properties of surfactant-free 80nm aluminium-oxide (alumina, Al_2O_3) spheroid gamma nanoparticle dispersions in 99.8% purity ethylene glycol (EG). Samples were diluted into 1, 2.5 and 5% by volume concentrations and pumped through an innovative purpose-developed thermally controlled closed system. Contrary to most studies which focus on individual property analysis through static burst (i.e. short term) data acquisition, concurrent data acquisition was achieved for relatively long testing periods, from 24 to 72 hours. This novel multifaceted approach also permitted to observe the long term effects of heat on colloid stability as well to insure repeatability of the data when applicable.

INTRODUCTION

For more than a century, scientists have been investigating the thermal characteristics of fluids containing solid particle dispersions. Maxwell [1] first postulated that a two-phase -i.e. fluid-solid- mixture would offer enhanced thermal conductivity by the influence of both quantitative and qualitative properties of the solid dispersed in the continuous phase, the base fluid.

Increasing needs in hyper-precise manufacturing processes and the emergence of nanotechnologies induced the development of nanofluids; a term coined by Choi et al. [2] for nanometer scaled two-phase colloids. Thermodynamic literature throughout the 1990s, motivated by Maxwell's medium effective theory, sought to study nanofluids to determine their viability in thermal applications, i.e. any appreciable thermal conductivity enhancement versus the mixture's base fluid. Novel research in the field indicated some anomalous thermal response and performance for low concentration nanofluids which increased the likelihood of enhancing current fluid cooling technology with the aid of nanoparticle dispersions.

To determine the viability of colloid nanodispersions in thermal applications and to further pursue into understanding nanofluid behaviour, general consensus of nanometer-scale thermal and rheological theories is essential. Experimental data acquisition is required for such progress by means of confirming or invalidating pertaining theories. However, nanofluid properties are characteristically difficult to normalize.

Indeed, as the inception of nanofluid interest created an appreciable body of data on the subject, the release of versed experimental studies has brought forth some contradictions to early literature. While it can be attributed to the steady refinements in nanoparticle manufacturing processes through the last decade, the presence of apparent inconsistencies in recent independent data over similar nanofluid types shows the influence of the experimental manipulation over data integrity. The International Nanofluid Property Benchmark Exercise [3], a scientific collaboration, was thus instated to gather methodologically-controlled mass data on the subject. The undertaking proved successful in establishing thermal

NOMENCLATURE

k	[W/mK]	Thermal conductivity
n	[-]	Form factor
V	[mL]	Volume
Special characters		
μ	[cP]	Dynamic viscosity
ϕ	[-]	Volume fraction ratio
Ψ	[-]	Ratio of area of particle and sphere of same V
Subscripts		
f		Continuous phase / Host fluid
m		Mass ratio
nf		Nanofluid
p		Solid phase / Nanoparticles
$prime$		After manipulation / Requested
rel		Relative ratio of property
v		Volume ratio
+		Required

conductivity standards for a few two-phase water nanofluid sample types, thus reinstating the need for thorough control of methodology and nanodispersion quality.

Conjointly, nanofluid research conducted on the colloid's chemical properties exhibited evidence of influence of physical and ionic stability over the thermal and rheological properties. For example, the host fluid acidity has been shown to influence the solid-phase's stability, as acidity chemically affects the surface charge of the particles [4]. Having a low ionic charge or uneven ionic distribution may cause degeneration of the solid phase, creating wide-spread agglomeration, which adversely affects the nanofluid's structure and properties.

In the present work, an analysis of a yet-studied commercially sourced 80nm spheroid Al_2O_3-EG surfactant-free nanofluid was performed through the use of a thermally-controlled closed circuit. The nanofluid's median nanoparticle size distribution (PSD) was determined through laser diffraction methods by the GRESPI laboratory at the Université de Reims Champagne-Ardenne. New thermal and rheological data was collected for the heating of samples in 1, 2.5 and 5% particle volume fractions. Analysis integrity was ensured through a thorough system validation, consistent analysis methodology and nanofluid pH control. Data obtained during a long term (24h+) heating period also allowed to observe colloid stability throughout the trials, a novel feature that had not yet been undertaken the field.

PROPERTIES OF NANOFLUIDS

A. Thermal Conductivity. Breakthrough research in nanofluids and their potential in thermal applications were first attributed to Masuda et al. [5] in which he demonstrated an anomalous thermal conductivity enhancement of the base fluid when mixed with a solid nanoparticle phase. Subsequent research results, even if most reported properties are supra-nominal to conjecture, reinforced the basis of Maxwell's medium effective theory in which a two-phase fluid's thermal conductivity is affected by qualitative (thermal conductivity; k) and quantitative (concentration; ϕ) characteristics of its solid phase:

$$k_{rel} = \frac{k_{nf}}{k_f} = \frac{k_p + 2k_f + 2(k_p - k_f)\phi}{k_p + 2k_f - (k_p - k_f)\phi} \quad (1)$$

Hamilton and Crosser [6] improved upon the model by integrating a form factor (n) over the spheroid solid phase. The form factor is determined by the equation $n=3/\Psi$ where Ψ is the ratio of the particle's surface area versus the area defined by a sphere of the same volume:

$$k_{rel} = \frac{k_{nf}}{k_f} = \frac{k_p + (n-1)k_f + (n-1)(k_p - k_f)\phi}{k_p + (n-1)k_f - (k_p - k_f)\phi} \quad (2)$$

Although other refinements to the equation exist, they are composed of highly specific terms which are not readily available without intrinsic knowledge of the studied sample's nanoparticle structure. Some also sought to validate and include theoretical rheological phenomena akin to Brownian motion into the model. While there is still debate over the effect of nano-scale phenomena between nanoparticles and their fluid host, Figure 1 summarizes what most agree are the key relations between spheroid nanofluids' thermal conductivity and their physical properties. For further insight, these properties were thoroughly reviewed by Wang et al. [7] and more recently Khanafer and Vafai [8].

Physical characteristic of nanofluid		k
Temperature of nanofluid	↗	↗
Volume of nanoparticles	↘	↗
Concentration of nanoparticle phase	↗	↗
Thermal conductivity of nanoparticles	↗	↗
Thermal conductivity of base fluid	↗	↗

Figure 1 Summary of the physical characteristics' influence on spheroid nanofluids' thermal properties

B. Dynamic Viscosity. The dynamic viscosity of nanofluids has been a rheological aspect that was met with limited interest. Typically, nanofluid viscosity was analysed at room temperature at different phase concentrations to determine if the colloid solid phase density dominated the reported thermal conductivity increase, essentially helping to qualify its viability in a real-world heat exchanging application and to fill physical parameters in simulation studies.

To have a true fundamental understanding of nanofluids, it is required to understand the full scope of the fluid's behaviour, both thermal and rheological, under thermal load. Understanding this, Pak and Cho [9] first published in 1998 the effect of temperature on the dynamic viscosity of TiO_2 and Al_2O_3 nanoparticles in water. Nguyen et al. [10] revised the subject with an analysis of Al_2O_3-water nanofluid dynamic viscosity under temperatures from 20°C to 75°C, from where they discovered that some of their higher concentration samples exhibited hysteresis when past a critical temperature threshold. The degradation of the affected nanofluid samples caused a permanent increase in dynamic viscosity that can likely be attributed to a wide-spread nanoparticle agglomeration through the liquid phase. Mintsa et al. [11] followed with an experimental investigation of the nanoparticle diameter's influence on the dynamic viscosity of two similarly based Al_2O_3-water nanofluids. Figure 2 shows a summary of these aforementioned reports on the dynamic viscosity (μ) of nanofluids.

Physical characteristic of nanofluid		μ
Concentration of nanoparticle phase	↗	↘
Thermal conductivity of nanoparticles	↘	↘
Thermal conductivity of base fluid	↗	↗

Figure 2 Summary of the physical characteristics' influence on spheroid nanofluids' dynamic viscosity

INSTRUMENTATION

A. Thermal Conductivity. The measurement of thermal conductivity of nanofluid samples in the system was accomplished by using the Decagon Devices KD2 Pro thermal properties analyser (Figure 3). A compact handheld device, the KD2 Pro is equipped with the optional KS-1 transient hotwire sensor capable of reading a fluid's thermal conductivity from 5°C to 150°C with a reported maximum deviation of 5%.

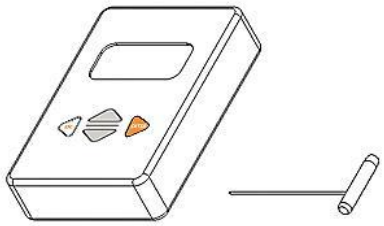

Figure 3 Decagon Devices KD2 Pro and KS-1 sensor

Prior to integration in the apparatus, the KD2 Pro was tested for accuracy. By bathing its sensor vertically in a glass jar of USP glycerine that was in turn completely submerged in a thermal control circulator's water bath tank, the laboratory was able to accurately test the KD2 Pro from 20°C to 70°C. The resulting trial showed that thermal conductivity readings impressively only deviated 0.3% from the tabulated values until 50°C. When the sample was heated over 55°C, micro-convection currents localized at the sensor's surface caused by natural heat flux in the static glycerine amplified the readings by 4.2%, nevertheless still within acceptable limits.

B. Dynamic Viscosity. The dynamic viscosity of the nanofluid samples was obtained by integrating an author-modified Cambridge Viscosity VISCOLab 4000 measurement cylinder (Figure 4) into the system. Dynamic viscosity analysis is achieved by the cylinder's magnetic field which pushes a piston through the shearing forces of the viscous sample fluid enclosed in the sealed measurement chamber, displaying readings of viscosity and inter-chamber temperature on the control box. Two measuring pistons were selected, one corresponding to a measuring range of 0.5-10cP (centipoise; $10cP = N{\cdot}s{\cdot}m^{-2} = kg{\cdot}m^{-1}{\cdot}s^{-1}$) scaled to the thousandth and the other to a range of 10-200cP scaled to the hundredth.

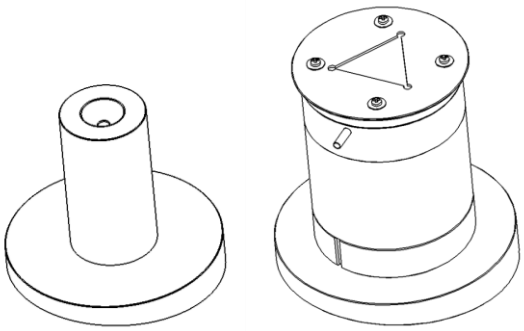

Figure 4 The apparatus's dynamic viscosity 'μ' module; Cambridge Viscosity VISCOLab 4000 measurement cylinder before (left) and after (right) modifications

Prior to the trials the manufacturer, stating that the instrument has a precision of 1% and an accuracy of 0.8% from -40°C to 100°C, recalibrated the unit to ISO 17025 factory references to ensure uncompromised analyses throughout the experimentation. Before assembling the modified cylinder module into the circulatory system, both ranges were tested at room temperature. The 0.5-10cP range was tested with Cambridge Viscosity's calibration fluid, labelled 'S3', which through viscous friction heating to 25°C deviated only 1.4% from the tabulated values. Because of a lack of manufacturer-sourced calibration fluid, the 10-200cP range was tested with fresh SAE 10w-30 motor oil and performed as expected with readings of approximately 130cP, its standard viscosity. Note that the use of a relative error cannot be justified considering that the manufacturer's formulation may differentiate slightly from the SAE's standard value.

EXPERIMENTAL APPARATUS

A. Apparatus. The novel concurrent data acquisition of the thermal conductivity and the dynamic viscosity of nanofluid samples requires a closed circuit that can both isolate the circulating sample from the environment and optimally integrate the instrumentation. To accomplish this task, a compact apparatus (Figure 6) was designed to complement the use of a heat exchanger (HX); a copper tube coil submerged into a Julabo thermal control circulator's bath tank. The thermal control circulator is equipped with a digital module, displaying the current bath temperature and regulating the heating coil/refrigerator for the system to reach a desired temperature.

The sample is first introduced into the thermal conductivity module (Figure 5), the triple-insulated reservoir. A vertically hollowed solid acts as a static mixer and increases the reservoir's wetted height, reducing the necessary fluid volume for testing. The design also minimises fluid vibrations when static and insures that the KD2's sensor, inserted horizontally into the reservoir, is adequately wetted throughout the trials. The horizontal position of the probe was favoured through the use of numerical and experimental simulations, as it inhibited the formation of localized convection currents.

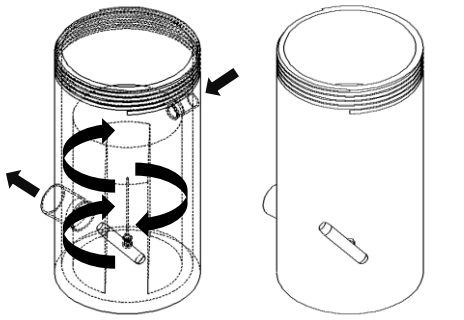

Figure 5 The apparatus's thermal conductivity 'k' module; a combination of the reservoir and the KD2's probe

The fluids are pumped from the reservoir, through the flow regulation valve and rerouted to the HX for temperature control. Thereafter, it reaches the dynamic viscosity module,

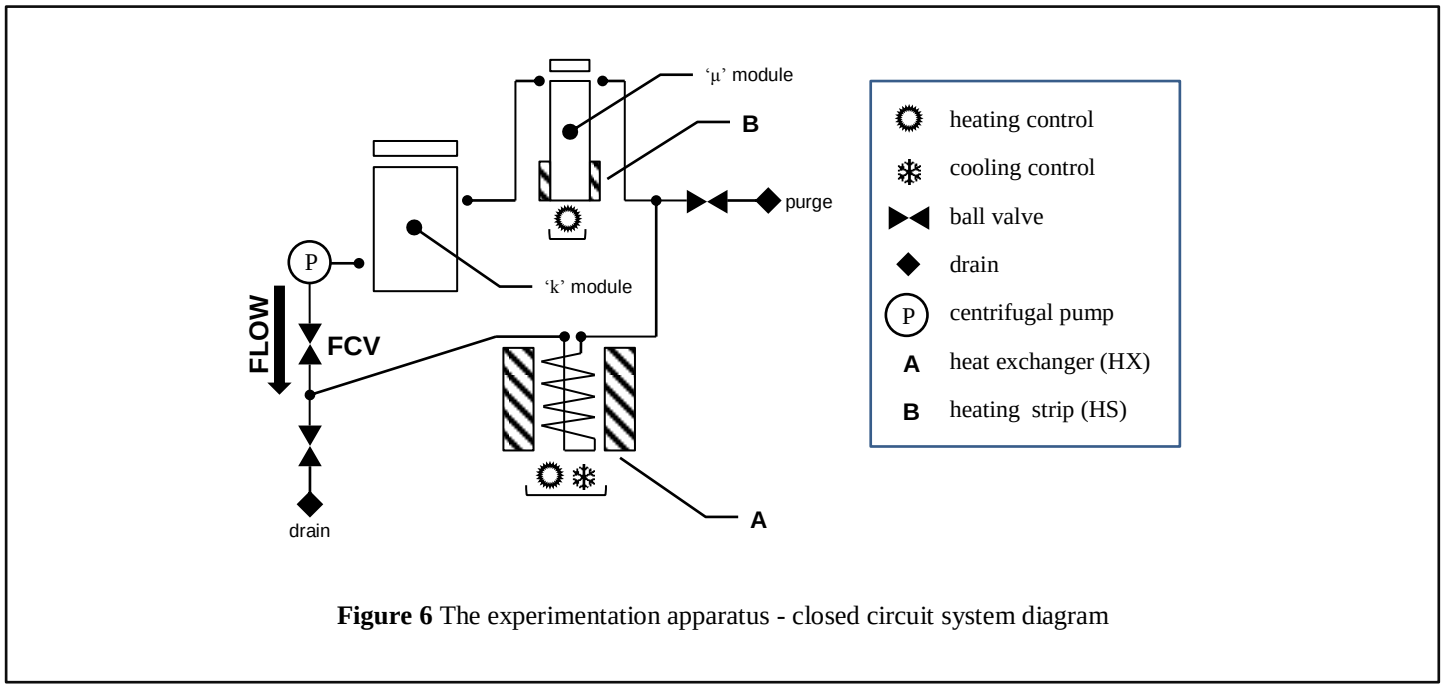

Figure 6 The experimentation apparatus - closed circuit system diagram

passing through its internal chamber and returning to the reservoir for cycle continuity. To accelerate the sample heating and to maintain sample internal heat for high temperatures, the VISCOLab 4000 measurement chamber is surrounded by a rheostat-controlled 17.5W silicone flexible heater (referred to as heating strip; HS). The module was also wrapped with two layers of insulation foam after assembly.

Most of the internal circulatory system, excluding the brass regulating ball valves, stainless steel sample reservoir and the 'μ' module's aluminium internal chamber, was composed of polyethylene or other resilient polymers to reduce internal sample contamination. Moreover, the small chemical-handling centrifugal pump was selected for its inert internal components and sized accordingly as per the manufacturer's reported flow versus pressure diagrams.

B. Sample preparation. The tested Al_2O_3-EG nanofluid samples were prepared in 500mL bulk by diluting the commercially sourced 20% mass concentration (%w/w) base Al_2O_3-EG mixture with laboratory grade anhydrous 99.8 purity ethylene glycol into fluid samples of 1, 2.5 and 5% particle volume concentrations (%v/v). Prior to dilution, the bulk nanofluid mass concentration ϕ_m must be converted to volume concentration ϕ_v. The latter is found by the use of equation (3). Both it and equation (4) were conceived by the author to streamline the sample preparation. The volume densities of the solvent fluid ρ_f and the nanofluid ρ_{nf} are required; the latter can be simply determined by weighting a defined volume of nanofluid. With ϕ_v known, the quantity of solvent fluid necessary (V_{f+}) to bring the desired dilution concentration (ϕ_{v_prime}) to the desired bulk volume (V_{nf_prime}) can be obtained:

$$\phi_v = 1 - \frac{\rho_{nf}}{\rho_f}(1 - \phi_m) \qquad (3)$$

$$V_{f+} = \frac{V_{nf_{prime}}(\phi_v - \phi_{v_{prime}})}{\phi_v} \qquad (4)$$

Ensuing dilutions of the 500mL bulk nanofluid samples were mechanically mixed, pH tested to the manufacturer's recommended values and sealed in LDPE containers before testing.

METHODOLOGY

A. Progressive heating. During system standby, the circulatory system's lowest level is filled with base fluid, typically spent ethylene glycol, to curb formation of granular oxide deposits in the copper coil of the HX. The preliminary preparation for analysis requires that the closed circuit be primed with sample nanofluid and that HX contaminates be evacuated. To do so, the flow control valve (FCV) is closed and the reservoir is filled with sample nanofluid; the combined activation of the pump and venting of the FCV creates a surge which flows through the HX, expulsing stagnated wastes. The contaminated cusp of the resulting flow is then rerouted through the inline purge valve located between the 'μ' module and the heat exchanger. Approximately 100mL of purge fluid has to be extracted to achieve satisfactory waste removal. Following the circuit purge, the system becomes fully operational. With the nanofluid readily flowing through the circuit at room temperature, the HX is set to ~25°C, the HS is set at minimum to preheat the electrical resistances and the FCV is maintained fully open to compensate for pumping losses caused by viscous friction. First levy occurs when the 'k' module and the 'μ' module report a sample temperature of 25°C. If not, adjustment of HX and/or increase of HS power are necessary to correct the sample's temperature.

Both the thermal conductivity and the viscosity require to be read while the fluid is stagnant, requiring the pump and FCV

to be completely shut off. When the operator is confident that residual vibrations in the reservoir have been dissipated, multiple KD2 Pro readings are taken to better converge the thermal conductivity to its lowest average, analogous to a low-pass signal filtration technique. For the dynamic viscosity measurement, precautions must be taken as the nanofluid sample confined within the measuring chamber appears highly sensitive to nanoparticle agglomeration, because of local turbulences. Thus, the 'μ' module's lid is unscrewed and the fluid in the chamber is extracted and immediately refilled (for high concentration samples) or thoroughly mixed (for low concentration samples) before inserting the appropriate piston to begin the viscosity measurement.

By repeating the aforementioned procedure at 5°C intervals the effect of temperature from 25°C to 65°C on the 1% 80nm Al2O3-EG sample and from 25°C to 55°C on the 2.5 and 5% samples was recorded, completing the primary objective of the study.

B. Prolonged heating. The trial consists of extending the heating phase when the sample reaches 55°C, which is the approximate temperature threshold of hysteresis reported by Nguyen et al. for high concentration (higher than 5%) Al_2O_3-water nanofluids. Hence at a temperature of 55°C the system's heating parameters are stabilized for steady state analyses which are levied at intervals of .5h, 1h, 2h, 6h, 12h and 24h. Utilizing the same measurement procedure as described for the progressive heat soak trial, the sample's sensitivity to long term heat soak can be directly observed, effectively completing the secondary objective of the study.

It should be noted that the first 15 to 30 minutes of the steady state heating usually consists of adjusting the HX and HS to compensate for environmental heat losses as they become more accentuated because of the higher temperature gradient with respect to the surrounding environment.

VALIDATION OF METHODOLOGY

To assess the integrity and accuracy of the data extracted from the closed system, three validations (V1, V2 and V3) were executed with fresh 99.8% purity ethylene glycol prior to the study. Figures 7 and 8 show grouped results for analyses of dynamic viscosity and thermal conductivity, respectively. It should be noted that sample V2's analysis suffered from an abrupt termination caused by circulatory leaks induced by heat and pressure fatigue on some components. All detected faults were detected and serviced appropriately prior the study.

The apparatus's 'μ' module proved to be very successful at matching theoretical sample viscosity throughout V1 to V3 testing while the 'k' module's results show the effect of convection currents on the probe during sample analysis. Being the same fluid levied from the 'μ' module, the 'k' module data acquisition quality and methodology can be deemed uncompromised. The aberrant trajectory given by the 'k' module's data trend is likely an effect of higher temperatures on the dynamic viscosity of the fluid, which reduced its ability to dampen convection currents and vibrations localized at the sensor's surface. Hence, the resulting convection factor on the sensor's probe at high temperatures artificially increases the static thermal conductivity that is being reported by the instrument. Careful considerations should thus be taken when interpreting thermal conductivity results at high temperatures.

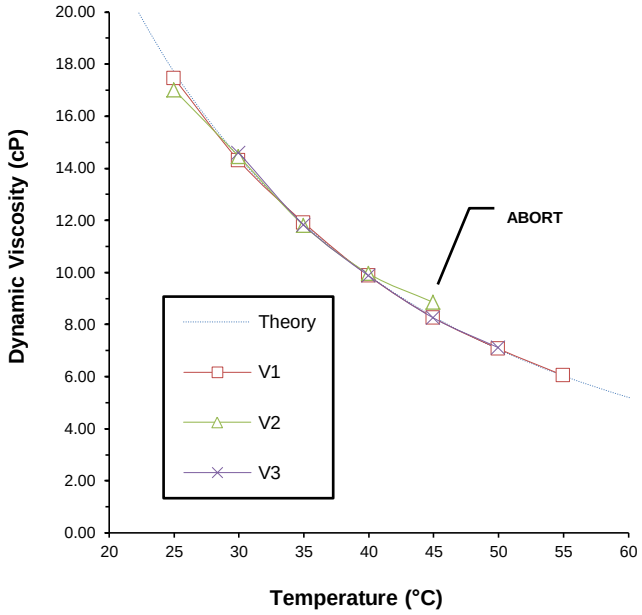

Figure 7 The apparatus's dynamic viscosity 'μ' module validation

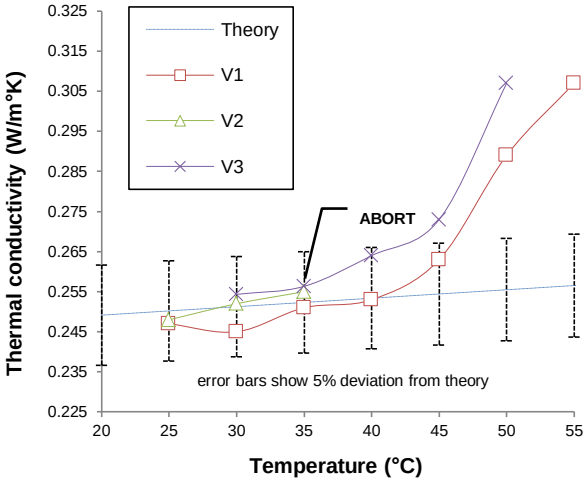

Figure 8 The apparatus's thermal conductivity 'k' module validation

RESULTS AND DISCUSSION

A. Data interpretation. To determine an appropriate regression for each data set acquired from the experimentation, criterions were established. For a nanofluid trend pattern to be physically plausible, the regression type cannot intersect the host fluid's function, as it would mean a violation of Maxwell's medium effective theory and other acknowledged generalized nanofluid behaviour. Thus, regressions with 20 point extrapolation of the functions' extremities that met the criterion

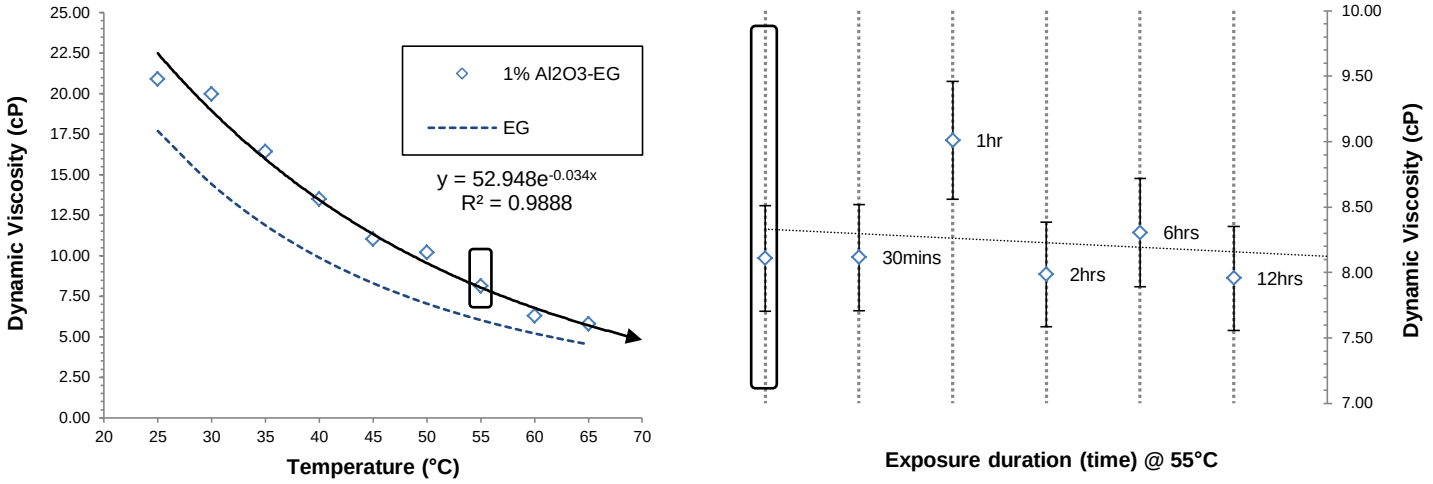

Figure 9 Dynamic viscosity of 1% Al_2O_3-EG nanofluid during progressive heating and prolonged heating at 55°C

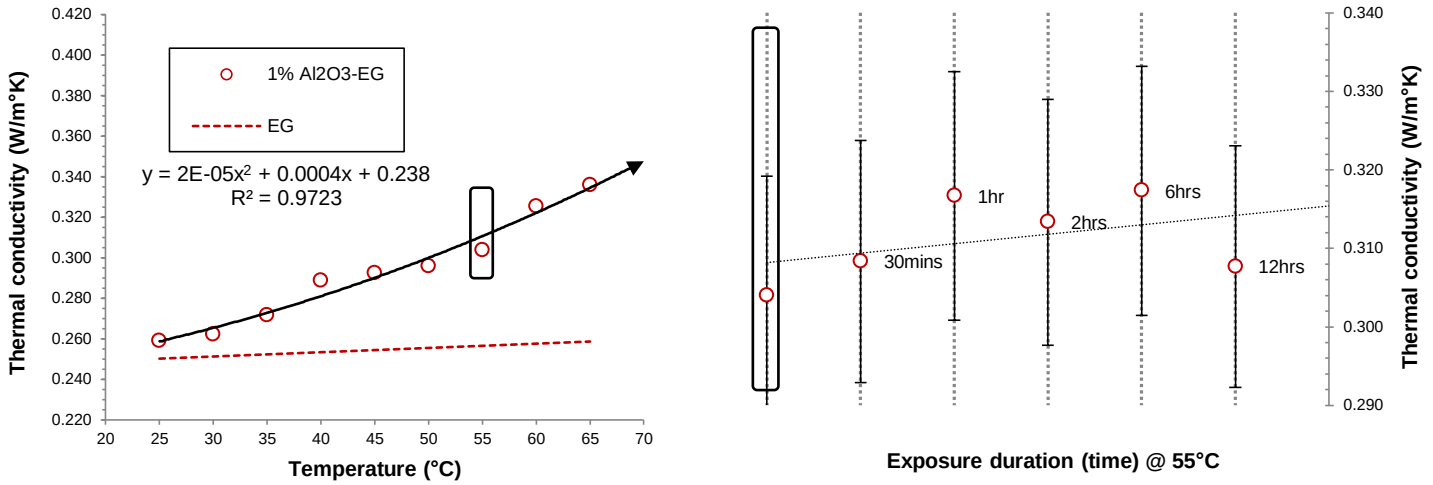

Figure 10 Thermal conductivity of 1% Al_2O_3-EG nanofluid during progressive heating and prolonged heating at 55°C

were deemed satisfactory. Moreover, the regressions' fitting qualities were underlined by the coefficient of determination R^2 (R square).

For posterity and interpretation consistency, discussed effects of temperature on the studied nanofluid sample use values from the fitted functions.

B. 1% 80nm Al_2O_3-EG. The apparatus behaved as expected, yielding data for the temperature's effect on thermal conductivity (figure 9) and viscosity (figure 10) of 1% 80nm Al_2O_3-EG nanofluid. The results have been graphically separated by experimentation phases where the left portion presents the gradual heating trial results and the right portion consists of a scaled timeline demonstrating the colloid stability under the extended heating exposure at 55°C. The magnitude of the y-axis scaling in the timeline is represented by a rectangle surrounding the 55°C data point in the progressive heating trial (left of figure) which is appropriately scaled in the prolonged heating time line (right of figure). It should be noted that the stability of the 1% v/v colloid at 55°C warranted the pursuit of the progressive heating study by extending the tests to 65°C.

The progressive heating trial demonstrates that the dynamic viscosity of the sample can follow a trend similar to an exponential degeneration of $y=52.948e^{-0.034x}$, x being the fluid temperature in °C, with R^2 = .9888. The fitting quality is also compounded by its quasi-constant phase with ethylene glycol's dynamic viscosity. Hence, at 25°C the 1% solid phase of the sample exhibited a 28% increase on the base fluid dynamic viscosity for only 4% improvement in thermal conductivity. The heating of the sample to 55°C caused a 64% decrease in dynamic viscosity, 33% over that of the base fluid. The thermal conductivity's trend fits the $y=2E(-5)x^2+0.0004x+0.328$ polynomial expression with an R^2 = .9723. The anomalous effect of temperature on the nanofluid's thermal conductivity evidently presented itself in the analysis, describing a wedge phasing between the nanofluid and its host fluid. Indubitably, Maxwell's medium effective theory for solid-fluid mixtures, exempt of any temperature-dependent parameters, implies that both phases should characterize proportionally the colloid's properties. However, pure alumina's thermal conductivity is degenerative under heating and ethylene glycol is ill-receptive

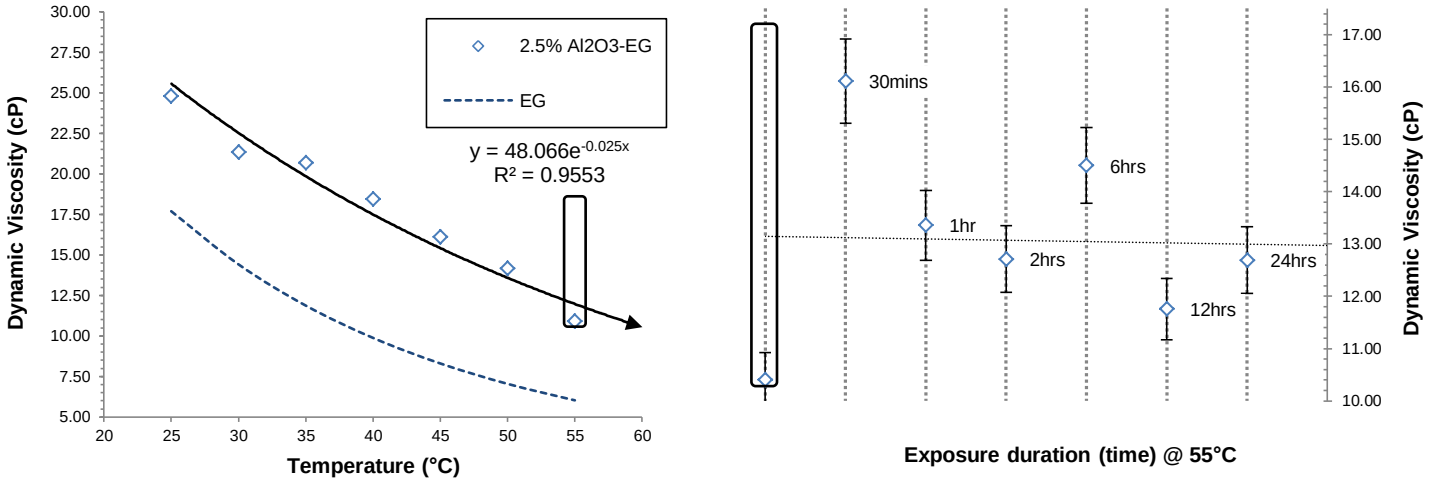

Figure 11 Dynamic viscosity of 2.5% 80nm Al_2O_3-EG nanofluid during progressive heating and prolonged heating at 55°C

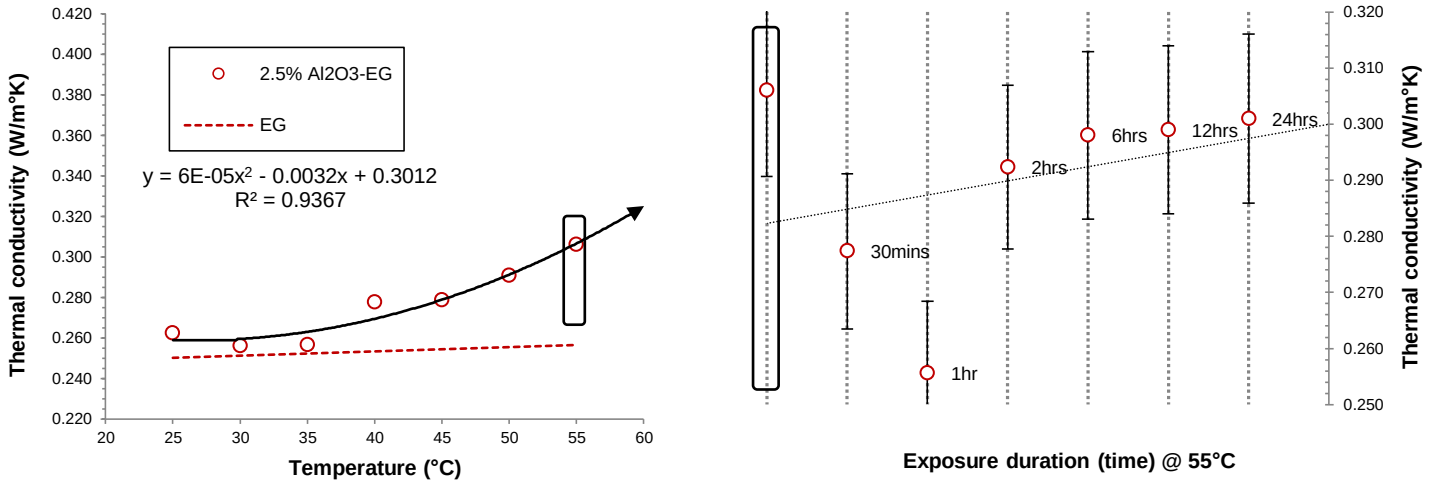

Figure 12 Thermal conductivity of 2.5% 80nm Al_2O_3-EG nanofluid during progressive heating and prolonged heating at 55°C

to temperature change. Therefore the nanofluid is exhibiting an unpredictable behaviour through yet-understood nanoscale rheological factors and can be surmised as experiencing an anomalous thermal enhancement, being affected by its solid phase through a temperature-sensitive process. Consequently, a 17% enhancement in thermal conductivity was observed from 25°C to 55°C, yielding a thermal conductivity 21% higher than ethylene glycol.

As stated, the perpetuated heating trial demonstrated that no appreciable degradation of properties was detected over the course of 12 hours. In fact, the slope of the thermal conductivity data's linear regression is less than the KD2 pro's reported deviation. The 5% error bars of the exposure duration graph also show the high data integrity throughout the trial, aside from the 1hr levy where the dynamic viscosity deviated farther than 9% from the linear trend. Given the consistency of the data contained in both timelines, the stray data point may be considered abhorrent and of no consequence to the study.

B. 2.5% 80nm Al_2O_3-EG. The dynamic viscosity regression (Figure 11) for the 2.5% sample shows a similar phasing to the 1% density sample, albeit at higher magnitude, and also fits a decaying exponential function; $y=48.066e^{-0.025}$ with an R^2 of .9553. At 25°C, the dynamic viscosity of the sample had been increased 46% over the base fluid by its solid nanoparticle phase. Heating the sample to 55°C reduced the shear rate by 50%. Despite of this, the addition of the solid dispersion rendered it 108% more viscous than its pure ethylene glycol phase at the same temperature.

The underlining effects of the 2.5% nanoparticle density and temperature on the thermal conductivity (Figure 12) is more pronounced than the 1% sample, as the regression exhibits signs of hyperbolic evolution with the curve-fitting polynomial function $y=6E(-5)x^2+0.0032x+0.3012$, R^2 = .9367. Similarly to the 1% sample, the thermal conductivity is approximately 4% superior to ethylene glycol at 25°C. Coincidentally, at 55°C the property had also increased by 17%, bringing it to 21%.

The 24 hours perpetuated heating trial presented some important deviation in both the 'k' and 'μ' module during the first hour. Hypothetically, a higher dispersion concentration

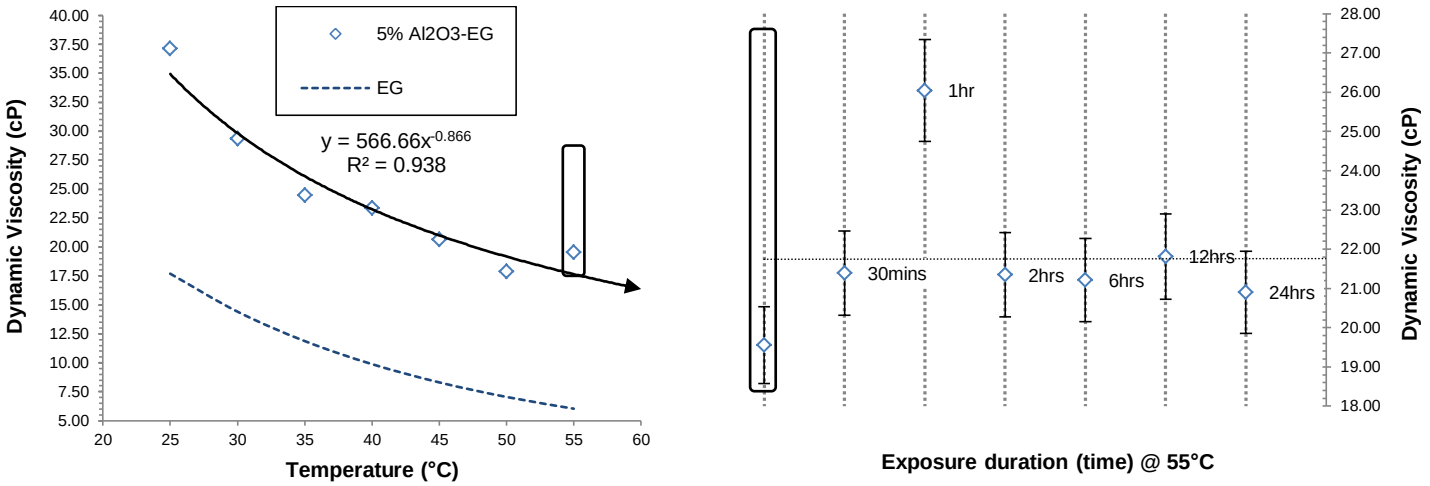

Figure 13 Dynamic viscosity of 5% 80nm Al_2O_3-EG nanofluid during progressive heating and prolonged heating at 55°C

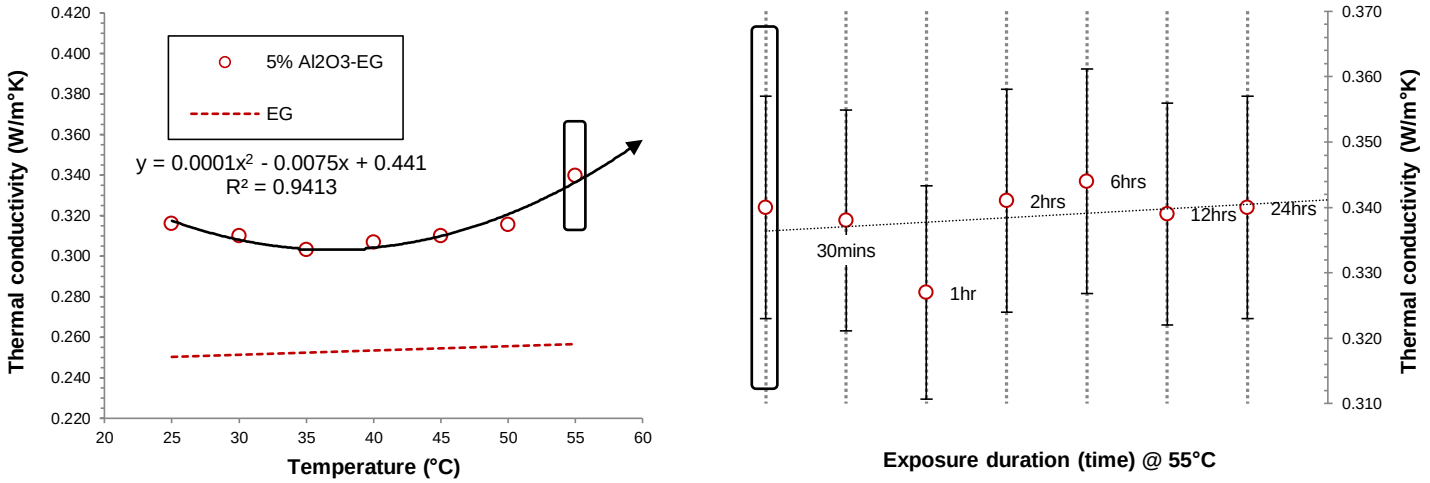

Figure 14 Thermal conductivity of 5% 80nm Al_2O_3-EG nanofluid during progressive heating and prolonged heating at 55°C

likely leads to a higher statistical probability of electromagnetic interfacial bonds forming through the metalloid dispersion. If the 2.5% colloid is less electromagnetically stable than its 1% predecessor, the oscillating data points could be attributed to a degeneration of the nanoparticle size distribution and homogeneity of the nanofluid triggered by the latent heating. The strong possibility of the properties undergoing hysteresis during the extended heating should thus be investigated. In consequence, the bulk of the sample was stored for posterity.

C. 5% 80nm Al_2O_3-EG. The dynamic viscosity regression (Figure 13) again describes a higher magnitude phasing of the host fluid's trend. While the exponential regression adequately fitted the previous iterations, the data points expressed by this trial is more favourable to a power expression $y=556.66x^{-0.866}$, the latter resulting in a higher R^2 (0.938 versus 0.887). At 25°C, the nanofluid sample is relatively twice as thick as ethylene glycol. Likewise to its 2.5% concentration predecessor, the heating from 25°C to 55°C caused a 50% reduction in its dynamic viscosity. At 55°C, it is approximately three times more viscous than ethylene glycol.

The effects of the solid phase on the thermal conductivity (Figure 14) in the 5% nanofluid are unexpected as the data points developed a full hyperbolic tendency with its vertex, i.e. point of symmetry, located near 35°C. This phenomena is described by a R^2 = 0.9413 factor fitting of the polynomial expression $y=0.0001x^2-0.0075x+0.441$. Hence, the sample showed an improvement upwards of 28% at 25°C oddly followed by a downward slope, bringing the proportion down to 20% at the trend's 35°C turning point. The ensuing heating to 55°C heightened the final reading to a 34% enhancement of the ethylene glycol.

Similarly to the 2.5% concentration sample, both the thermal conductivity and dynamic viscosity resulting from the perpetuated heating trial show some oscillatory behaviour during the first hour levies, although ultimately stabilizing around the median. Given the similarity of the pattern to the 2.5% Al2O3-EG's trial and the inherent statistical implications of its high nanoparticle concentration on colloid stability, the sample's bulk was also stored for future research.

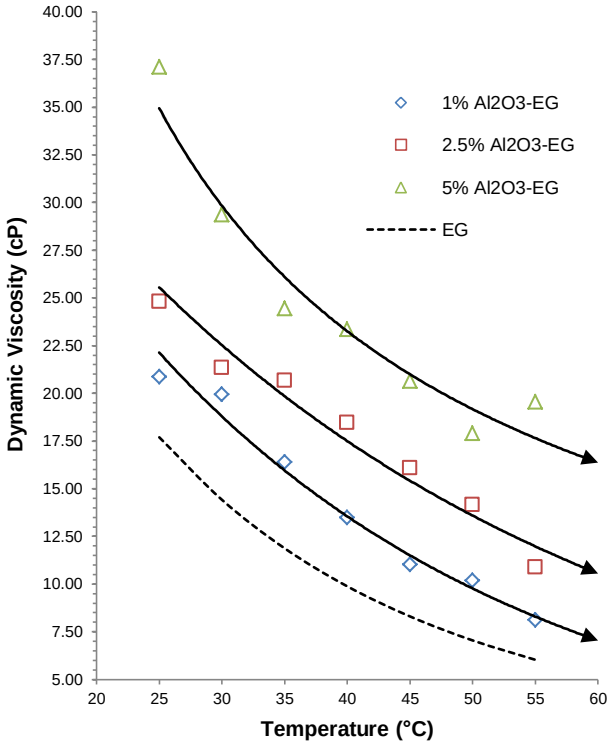

Figure 15 The effect of dispersion density on the dynamic viscosity of 80nm Al_2O_3-EG nanofluid

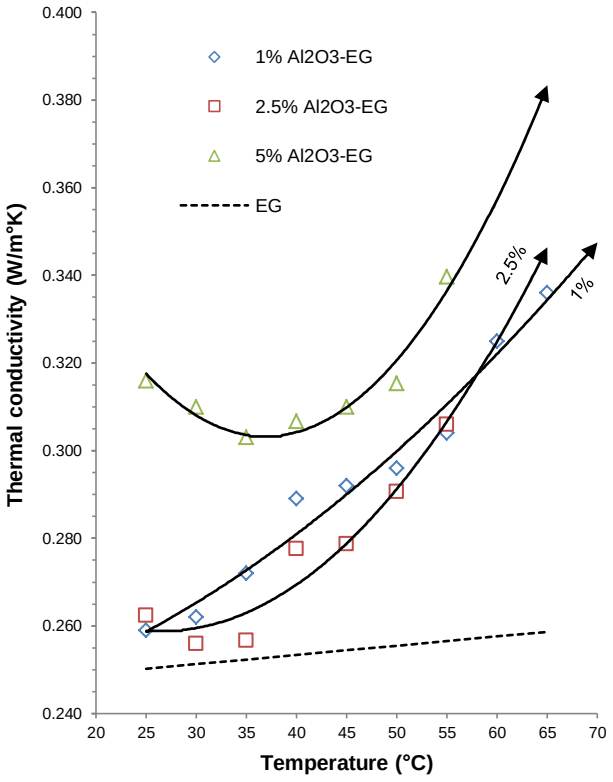

Figure 16 The effect of dispersion density on the thermal conductivity of 80nm Al_2O_3-EG nanofluid

D. Discussion. In the interest of observing the effect of nanoparticle concentration on Al_2O_3-EG nanofluid properties, the data for dynamic viscosity and thermal conductivity of all three concentration samples were superimposed. The dynamic viscosity regressions (Figure 15) clearly show that the nanofluid's rheological property is highly dependent of the host fluid, as a constant phasing with the ethylene glycol's trend for all samples indicate that the nanodispersion's contribution to the property is seemingly unaffected throughout the temperature range.

Although the literature agrees that the thermal conductivity should be proportional to the nanofluid concentration, Figure 16 demonstrates that from 25 to 57°C the 2.5% hyperbole regression is lower on the y-axis than the 1% sample. Beyond 57°C, the 2.5% sample's steep evolution overtakes the linear 1% sample as expected from the generalized convention.

Regarding the stability of the tested nanofluids, it is comprehensible that an extended heating exposure on samples that contain a sufficiently high solid phase concentration, e.g. 2.5%, at high temperatures increases the statistical likelihood of successful bonding collisions between nanoparticles, in turn causing the degeneration of the suspension through agglomeration. The sample's degradation in steady state heating seems to cause an erratic modification of their dynamic viscosity and of their thermal conductivity. This behaviour, believed to be observed for the first time, would raise serious concerns regarding the application of these fluids in practical thermal exchange applications.

CONCLUSION

The data acquired from the study will contribute to the existing body of work for nanofluids, including data for yet-studied 80nm scale nanoparticles and their steady state stability. The multifaceted experimental approach performed as expected, likely constituting the first published report of the kind in the field. Moreover, the use of a transient state and steady state for a temperature dependency study permitted to accurately observe the prolonged heating effects on colloid stability, a feature that was also missing in literature. While academic interest sought to analyse a range of surfactant-free 80nm Al_2O_3-EG nanofluid samples in 1, 2.5 and 5% concentrations, the high dynamic viscosity and low stability of 2.5 and 5% 80nm Al_2O_3-EG may outweigh their enhanced thermal conductivity in certain practical applications. It would also be of interest to future research to seek a proper understanding of their thermal conductivities' hyperbola progression and the mechanisms that are influential to their formation.

ACKNOWLEDGMENT

This project is part of the R&D program of the NSERC Chair in Industrial Energy Efficiency established in 2006 at the *Université de Sherbrooke*. The authors acknowledge the support of the Natural Sciences & Engineering Research Council of Canada, Hydro Québec, Rio Tinto Alcan and Canmet-Energy Research Center of Natural Resources Canada, and the *Université de Moncton*'s Faculty of Engineering.

REFERENCES

[1] Maxwell, J.C. A Treatise on Electricity and Magnetism, 2nd edition, Claredon, U.K., 1881

[2] Lee, S., Choi, S.U.S, Li, S., Eastman, J.A., Measuring thermal conductivity of fluid containing oxide nanoparticles, *ASME Journal of Heat Transfer*, Vol. 121, 1999, pp280-289

[3] Buongiorno, J. et al.; INPBE A benchmark study on the thermal conductivity of nanofluids International Nanofluid Property Benchmark Exercise, *Journal of Applied Physics*, 2009, Vol. 106

[4] Wang, X., Xinfang, L., Yang, S. Influence of pH and SDBS on the stability and thermal conductivity of nanofluids, *Energy and Fuels*, Vol.23, 2009, pp2684-2689

[5] Masuda, H., Ebata, A., Teramarae, K., Hishinuma, N. Alteration of thermal conductivity and viscosity of liquid by dispersing ultra-fine particles, *Netsu Bussei*, Vol. 4, no. 4, 1993, pp227-233

[6] Hamilton, R. L., & Crosser O. K., Thermal conductivity of heterogeneous two-component systems, I&EC Fundamentals, Vol. 1, 1962, pp731-734

[7] Wang, X.-Q., Mumjumdar, A. S. Heat Conduction in nanofluids, *International Journal of Thermal Sciences*, Vol.46, 2006, pp1-19

[8] Khanafer, K., Vafai, K., A critical synthesis of thermophysical characteristics of nanofluids, *Int. J. Heat Mass Transfer*, 2011

[9] Pak, B.C., Choi, Y.I. Hydrodynamic and heat transfer study of dispersed fluids with submicron metallic oxide particle, *Experimental Heat Transfer*, Vol. 11, no. 2, 1998, pp151-170

[10] Nguyen, C.T. Desgranges, F., Roy, G., Galanis, N., Maré, T., Boucher, S.,Angue Mintsa, H. Temperature and particle-size dependant viscosity data for water-based nanofluids – Hysteresis phenomenon, *International Journal of Heat and Fluid Flow*, Vol. 28, 2007, pp1492-1506

[11] Mintsa, H.A., Nguyen, C.T., Roy, G.,Doucet, D. New temperature dependant thermal conductivity data for water-based nanofluids, *Int. J. of Thermal Sciences*, Vol. 48, 2009, pp363-371